Precipitation changes within dynamical regimes in a perturbed climate

ENVIRONMENTAL RESEARCH
LETTERS

PURPOSE-LED PUBLISHING™ Part of the ENVIRONMENTAL RESEARCH SERIES

OPEN ACCESS

Precipitation changes within dynamical regimes in a perturbed climate

To cite this article: Jonny Williams and Mark A Ringer 2010 *Environ. Res. Lett.* **5** 035202

IOP Publishing Environmental Research Letters
Environ. Res. Lett. **5** (2010) 035202 (8pp) doi:10.1088/1748-9326/5/3/035202

Precipitation changes within dynamical regimes in a perturbed climate

Jonny Williams and Mark A Ringer

Met Office Hadley Centre, FitzRoy Road, Exeter EX1 3PB, UK

E-mail: mark.ringer@metoffice.gov.uk

Received 15 January 2010
Accepted for publication 21 June 2010
Published 5 July 2010
Online at stacks.iop.org/ERL/5/035202

Abstract
Tropical precipitation and the character of its adjustment in response to climate warming have been examined in an ensemble of climate models. Partitioning the 500 hPa pressure velocity, ω, into four basic dynamical regimes reveals that areas which exhibit a reversal of ω from descent to ascent make a disproportionately large contribution to the total precipitation change. The four regimes' occurrences are remarkably consistent across the ten models considered but the inter-model spread of some of the precipitation changes is very large. This large variation is, however, primarily due to two of the models, IPSL and CCSM3. A further separation into 'dynamic' and 'thermodynamic' changes confirms that the inter-model spread in precipitation is related to variations in the dynamical responses of the models. The reliability of models for climate change studies can to some extent be gauged by their ability to represent present day climate variability. An example, using interannual variability, is presented for the Hadley Centre model, HadGEM1. This highlights potential strengths and weaknesses of the model regarding simulation of the relationships between precipitation, surface temperature, and the large-scale circulation.

Keywords: climate modelling, climate change, precipitation, hydrological cycle, dynamical regimes

1. Introduction

Working Group 2 of the IPCC 4th Assessment report (AR4) concluded that the frequency of heavy precipitation events is 'very likely' to increase under future climate change (Parry *et al* 2007, Allan and Soden 2008), where 'very likely' refers to a 90%–99% chance of this occurring. Working Group 1 of AR4 (Solomon *et al* 2007) pointed to a scientific consensus surrounding the strength of the global mean hydrological cycle, that is, the global mean total precipitation (Held and Soden 2006). The Clausius–Clapeyron relation relates the increase of saturation vapour pressure of the atmosphere to the temperature

$$\frac{\mathrm{d}e_\mathrm{s}}{\mathrm{d}T} = LR^{-1}e_\mathrm{s}T^{-2} \tag{1}$$

where e_s is the saturation vapour pressure, T is the temperature, L is the latent heat of vaporization and R is the gas constant. It has be shown that convective precipitation can be expected to increase at the same rate of roughly 7% K^{-1} (Allan and Soden 2007, Allen and Ingram 2002). The same is not true for total (the sum of convective and stratiform) precipitation, where the increase is predicted to be roughly 3–4% K^{-1} (Allan and Soden 2007). Therefore, the stratiform precipitation, on a global mean basis, is predicted to decrease.

This work attempts to provide a basis for investigation of precipitation changes as defined within specified dynamical regimes under climate change. It is found that small changes in the large-scale circulation can have a very large effect on the resultant precipitation changes. This has the corollary that simply understanding where the general circulation is expected to change is not enough to understand how precipitation patterns will themselves alter due to a highly non-linear response of the hydrological cycle. This has implications for potential mitigation of climate change impacts because those areas of the world which are predicted to suffer the most from a perturbed Earth system mostly lie within the

tropics, where the following data analysis (section 4) is carried out.

Analysis of precipitation changes in response to climate warming within dynamical regimes is performed by examining the 500 hPa pressure velocity as a proxy for the large-scale atmospheric circulation and its relation to the hydrological cycle. This is a commonly used technique (for example Bony *et al* 1997, Bony *et al* 2004, John *et al* 2009). In the tropics, due to conservation of mass, the 500 hPa pressure velocity is equivalent to using the horizontal wind divergence at 200 hPa or the convergence at 850 hPa (Hartmann and Michelson 1993). Using pressure velocity at 400 or 600 hPa also gives similar results (Vecchi and Soden 2007).

2. Observational data sets and model simulations

Before analysing multi-model simulations of precipitation changes under climate change, the atmospheric component of the most recent Met Office Hadley Centre model, HadGEM1 (Martin *et al* 2006) is examined in section 3. The validation data set for the precipitation in this study is the Global Precipitation Climatology Project (GPCP), version 2 (Adler *et al* 2003). CMAP data (Xie and Arkin 1997) and ERA-40 reanalysis (Uppala *et al* 2005) have also been used to separately validate the model results. The surface temperature data are from ERA-40; HadCRUT3 (Brohan *et al* 2006) data were used to check the results. The pressure velocity data are from the ERA-40 reanalysis; additional validation was performed using the NCEP reanalysis (Kalnay *et al* 1996).

Section 4 uses the atmospheric component of HadGEM1 coupled to a 50 m mixed layer (or 'slab') ocean (HadGSM1) and also compares this model with the slab ocean versions of HadCM3 (Pope *et al* 2000), HadCM4 (Webb *et al* 2001) and the mean of the remaining models in the Cloud Feedback Model Intercomparison Project (CFMIP) project, which formed part of AR4. The slab ocean versions of HadCM3(4) are know as HadSM3(4). Complete information on the CFMIP project can be found at www.cfmip.net. HadCM3 was the predecessor of HadCM4, which was in turn the predecessor to HadGEM1. There are significant differences between HadCM3 and HadCM4, many of which were then incorporated into HadGEM1. In comparison to HadCM3, HadCM4 and HadGEM1 include, for example, increased vertical resolution, a new boundary layer scheme (Lock 2001) and a parameterization for convective anvils. HadGEM1 additionally includes increased horizontal resolution and uses a new dynamical core employing semi-Lagrangian advection compared to the Eulerian dynamics used in HadCM3 and HadCM4. Full details of the differences between the atmospheric components of HadCM3 and HadGEM1 are in Martin *et al* (2006).

3. Model precipitation changes are strongly correlated with temperature and circulation

The fields used in this section are monthly mean anomalies from the mean seasonal cycle. The analysis is analogous to that used previously to examine the covariability of temperature and precipitation anomalies by Adler *et al* (2008) and Trenberth and Shea (2005). Before examining the changes in the character of precipitation brought about by a doubling of the concentration of atmospheric CO_2, the present day precipitation variability and its relation to surface temperature and the large-scale circulation are examined.

It is clear from figures 1(a) and 2(a) that the model's precipitation variability is too high compared to the GPCP data over the deep tropics and the South Pacific convergence zone (SPCZ). The variability of GPCP and CMAP data are similar, with CMAP showing a marginally increased variability in the equatorial west Pacific. The variability of the ERA-40 precipitation, however, is larger than either of the two observational datasets, although still lower than that from the model in the deep tropics. Large areas of low variability off the west coasts of Africa and South America are associated with areas of persistent non-precipitating low level cloud. In spite of the overestimated variability, the geographical pattern of rainfall variability is very well captured by the model. Figure 2(b) captures the distribution of figure 1(b) well but does slightly overestimate the magnitude, in agreement with the relation between figures 1(a) and 2(a).

The similarity between the distributions of precipitation variability and mid-tropospheric pressure velocity variability in the model and validation data indicates a strong link between rainfall changes and changes in the general circulation (see also Vecchi and Soden 2007). This is a key result and forms the basis of the work in section 4 where the relationship between precipitation changes and circulation changes under climate change is examined.

The correlations between precipitation and surface temperature anomalies in figures 1(c) and 2(c) show good agreement between the model and the validation data in terms of a strong positive ENSO correlation in the equatorial Pacific Ocean and negative correlations over large continental land masses, as noted previously in Trenberth and Shea (2005). In these latter regions, and on interannual timescales, the prevailing conditions are therefore warm and dry or cool and wet. The Arctic and Antarctic regions show poor agreement between the model and validation data, however, these regions are poorly constrained by observational data. The HadCRUT3 surface temperature data set has also been used to validate the model data. The conclusions reached are unchanged and ERA-40 is shown here because it is spatially complete. Overall, the magnitude of the correlation shown in figure 2(c) is an overestimate of that in figure 1(c), although with a good geographical distribution, demonstrating that the two variables under consideration here are more tightly coupled in the model than is observed.

The correlation between surface temperature and precipitation (figures 1(c) and 2(c)) are a combination of both locally and remotely forced responses. Examination of the effect of the SST in the Nino 3.4 region on global precipitation enables isolation of part of the remote response (e.g. Trenberth *et al* 2002), as shown in figures 1(d) and 2(d). In this case the agreement between model and validation data is good: the main difference is the inability of the model to reproduce the magnitude of the negative correlation in the SPCZ. It should

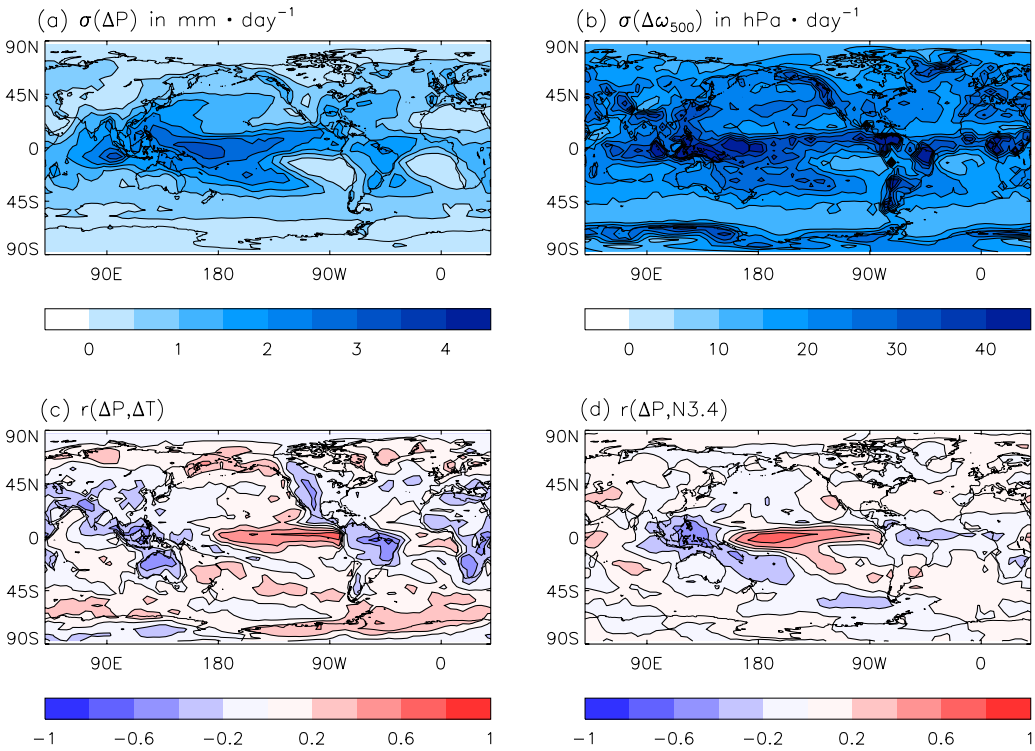

Figure 1. Validation data: (a) precipitation variability (standard deviation of the monthly mean anomalies), (b) 500 hPa pressure velocity variability, (c) local correlation between precipitation and 1.5 m temperature and (d) correlation between precipitation and average 1.5 m temperature in the Nino 3.4 region. Data are for 1979–2001 inclusive. The precipitation data set is GPCP and the (1.5 m) temperatures and pressure velocities are from the ERA-40 reanalysis.

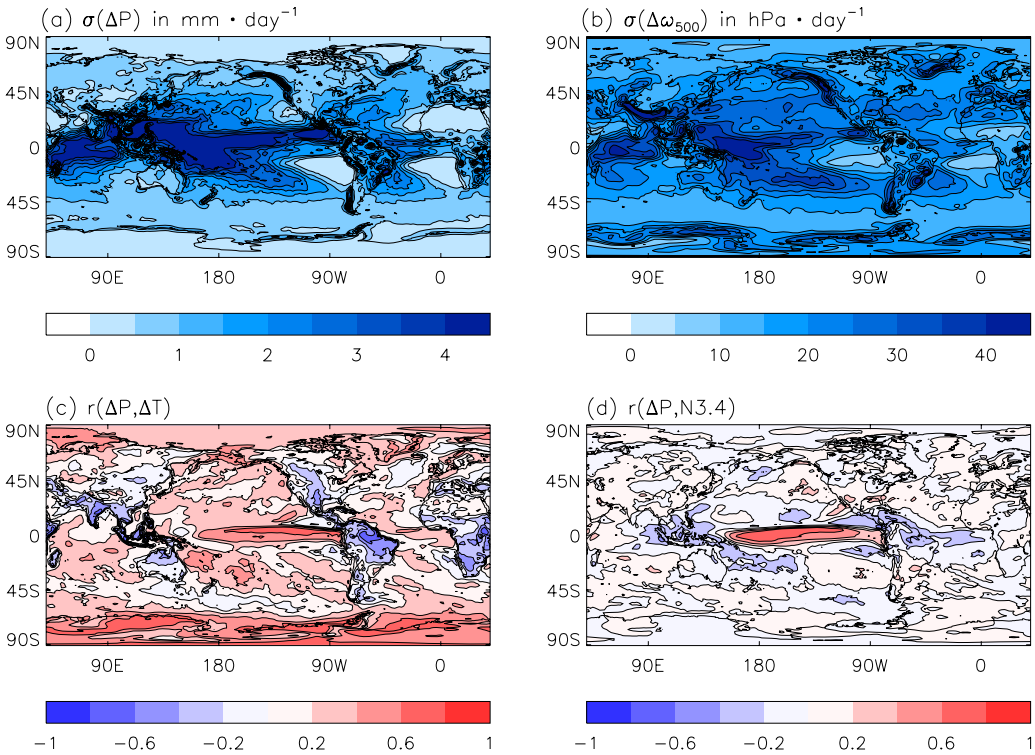

Figure 2. HadGEM1 model data: (a) precipitation variability, (b) 500 hPa pressure velocity variability, (c) local correlation between precipitation and 1.5 m temperature and (d) correlation between precipitation and average 1.5 m temperature in the Nino 3.4 region. Data are for 1979–2001 inclusive and are from a simulation using the atmospheric component of HadGEM1 forced with the observed distributions of SST and sea-ice.

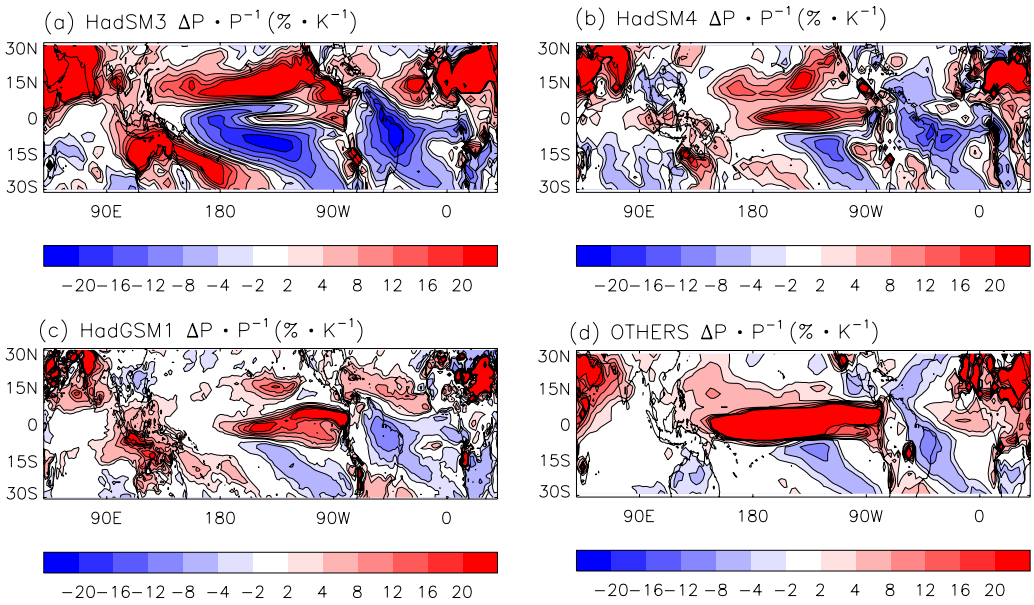

Figure 3. The percentage change in total precipitation, expressed as a fraction of the control, between the 2 × CO_2 and control simulations for (a) HadSM3, (b) HadSM4, (c) HadGSM1 and (d) the mean of non-Hadley centre CFMIP models ('Others'). The results for each model have been normalized by the appropriate global climate sensitivity.

be remembered that the model in this case uses prescribed SSTs and therefore is unable to simulate atmosphere–ocean feedback mechanisms which may play a significant role in this process (Trenberth *et al* 2002). While the correlations shown can provide useful insights it should be noted that they do not necessarily indicate the sign of any causal relationships between temperature and precipitation, which themselves may also vary from region to region.

To summarize, it is clear that the HadGEM1 model reproduces several important observed features of the present day hydrological cycle and that precipitation and the general circulation are intimately coupled. This has important implications for changes in the future hydrological cycle given that the general circulation is predicted to weaken under climate change (Vecchi *et al* 2006, Vecchi and Soden 2007). It is also apparent that this model (in common with other models submitted to AR4) also differs from the observed behaviour in potentially important ways; this always needs to be borne in mind when examining climate change simulations of similar relationships.

4. Partitioning variables into dynamical regimes enables isolation of the climate change signal

The climate change signals in HadSM3, HadSM4 and HadGSM1 are now examined, again using monthly mean data, and compared to the remaining seven models in the CFMIP project database. In this case, however, absolute monthly means are used, not anomalies. Steady state results from numerical experiments are compared in which the atmospheric CO_2 concentrations differ by a factor of two (280 cf 560 parts per million). Using the 500 hPa pressure velocity (ω), the climate change signal is divided into four large-scale circulation regimes.

(1) Ascent in control and 2 × CO_2, ω^{--}.
(2) Ascent in control, descent in 2 × CO_2, ω^{-+}.
(3) Descent in control, ascent in 2 × CO_2, ω^{+-}.
(4) Descent in both the control and 2 × CO_2, ω^{++}.

Vecchi and Soden (2007) and Emori and Brown (2005) both separated precipitation into its 'dynamic' and 'thermodynamic' components. Here the definition of the 'dynamical precipitation change' from Vecchi and Soden (2007) is used. The fractional increase in precipitation due to dynamical changes is then given by the difference between the precipitation change and the rate of Clausius–Clapeyron moistening:

$$\frac{\Delta P}{P} - 0.07\Delta T.$$

The first term is the fractional change in total precipitation and ΔT is the local surface temperature change. Physically, when the change in dynamic precipitation is negative, the increase in total precipitation is lower than the rate of increased moistening in the atmosphere predicted by the Clausius–Clapeyron relation.

Figure 3 shows the fractional changes in precipitation for each of the three Hadley Centre models as well as the mean of the seven other slab ocean models in the CFMIP archive (for these models we show the mean of the individual models' fractional changes in precipitation). Note that the patterns of these changes in precipitation are strongly correlated with those in ω (not shown—see also Vecchi and Soden (2007)). Figure 4 shows the equivalent data for the dynamical precipitation change. Where the fractional change in the dynamical precipitation is close to zero, the change in the total precipitation tracks the change in temperature (and hence atmospheric water content) and the influence of changes in the large-scale circulation is small. In all the

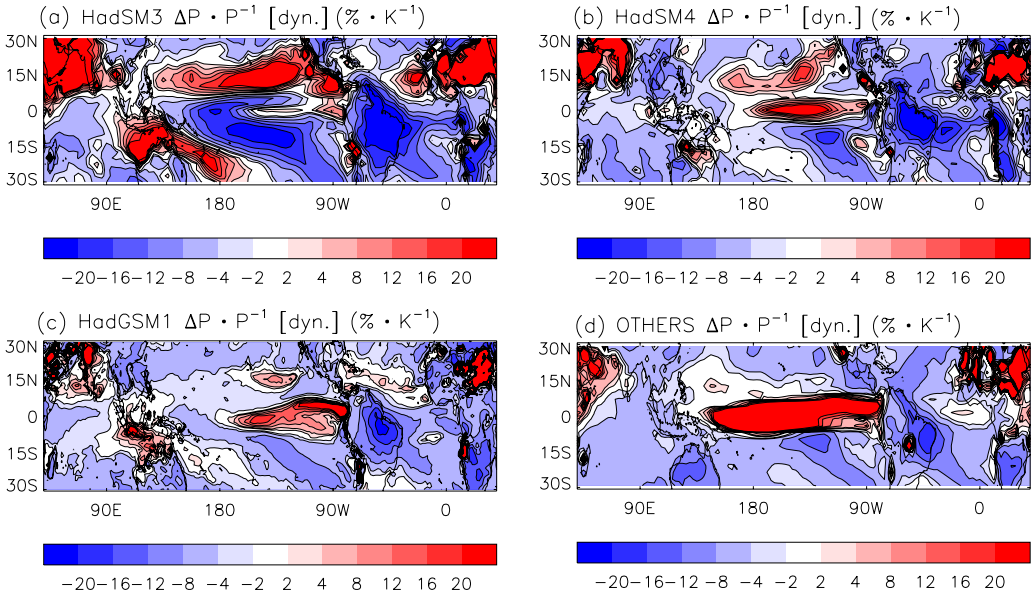

Figure 4. As figure 3 but for the dynamical precipitation changes.

models considered here, throughout the tropics, there are clearly significant changes in atmospheric circulation driving changes to the distribution of precipitation.

Figure 3(d) reproduces some of the main features of the ensemble mean shown in Vecchi and Soden (2007), particularly the large increase in precipitation over the equatorial Pacific Ocean. The agreement with the precipitation changes shown in Emori and Brown (2005), who used a somewhat smaller ensemble, is better however, additionally showing a noticeable decrease over the Amazon basin for example. Within the ensemble considered here there is significant inter-model variation. In particular, large positive values in the equatorial Pacific Ocean in figure 3(d) are strongly influenced by the responses of the CCSM3 and IPSL models. Figure 3(a) shows that HadSM3 is the most sensitive Hadley Centre model in terms of its total precipitation response, with HadGSM1 the least sensitive and HadSM4 being an intermediate case.

The overall behaviour of the dynamical precipitation change (figure 4) is similar to the total change, with the ensemble mean response over the equatorial Pacific Ocean being dominated by the CCSM3 and IPSL models and HadSM3 having the most sensitive response of the Hadley Centre models. HadSM3 also has larger areas where the dynamic precipitation changes are positive, which are absent in HadSM4, HadGSM1 and the mean of the rest of the ensemble.

Increasing the tropospheric resolution of HadSM3 (from 19 to 30 levels) does not change the results significantly. Therefore the origin of the differences between HadSM3 and the other Hadley Centre models is likely to be the different boundary layer scheme and its interaction with the convection scheme, with the further differences between HadSM4 and HadGSM1 being due to the increased horizontal resolution and interactions with the different dynamical core. Note that it is less straightforward to attribute the differences in global climate sensitivity to individual changes in the models as these arise due to a combination of many small effects (see Johns *et al* 2006 for further details).

Comparing figures 3(a) and 4(a), the fractional changes in total and dynamic precipitation for HadSM3 are very similar. This shows that the precipitation changes in HadSM3 are dominated by dynamical changes and suggests that the thermodynamic changes are small. The similarity is lessened when comparing figures 3(b) and 4(b), as well as figures 3(c) and 4(c), indicating that dynamical effects are weaker in HadSM4 and HadGSM1 and suggesting that the thermodynamic response, which can be deduced from the differences between figures 3 and 4, plays a larger role in these models. The same is true when considering the ensemble mean in figures 3(d) and 4(d), indicating that HadSM4 and HadGSM1 are more consistent with the mean of the rest of the CFMIP ensemble in this respect.

Figure 5 shows several quantities of interest with regard to precipitation changes over the tropical oceans. It is clear from figures 5(a) and (b) that although the regimes representing a change in sign of pressure velocity (ω^{-+} and ω^{+-}) occur relatively infrequently, they have a disproportionately large effect on the precipitation change. Their respective effects on the resultant precipitation, however, tend to cancel out for the Hadley Centre models, though clearly do not for the mean of the other models. Regime ω^{--} makes the largest contribution to the total precipitation change, tending to increase the rainfall, while regime ω^{++} has little net effect on the precipitation change, which is probably unsurprising given that the rainfall tends to be much lower in descending regimes.

Figure 5(c) shows that the regime representing descent in the control becoming ascent in the perturbed climate (ω^{+-}) is a significant driver of tropical precipitation changes. The other regime showing ascent becoming descent (ω^{-+}) shows the next largest fractional response, acting to decrease the fractional change in precipitation. The fractional change in precipitation in the regimes ω^{--} and ω^{++} show negligible

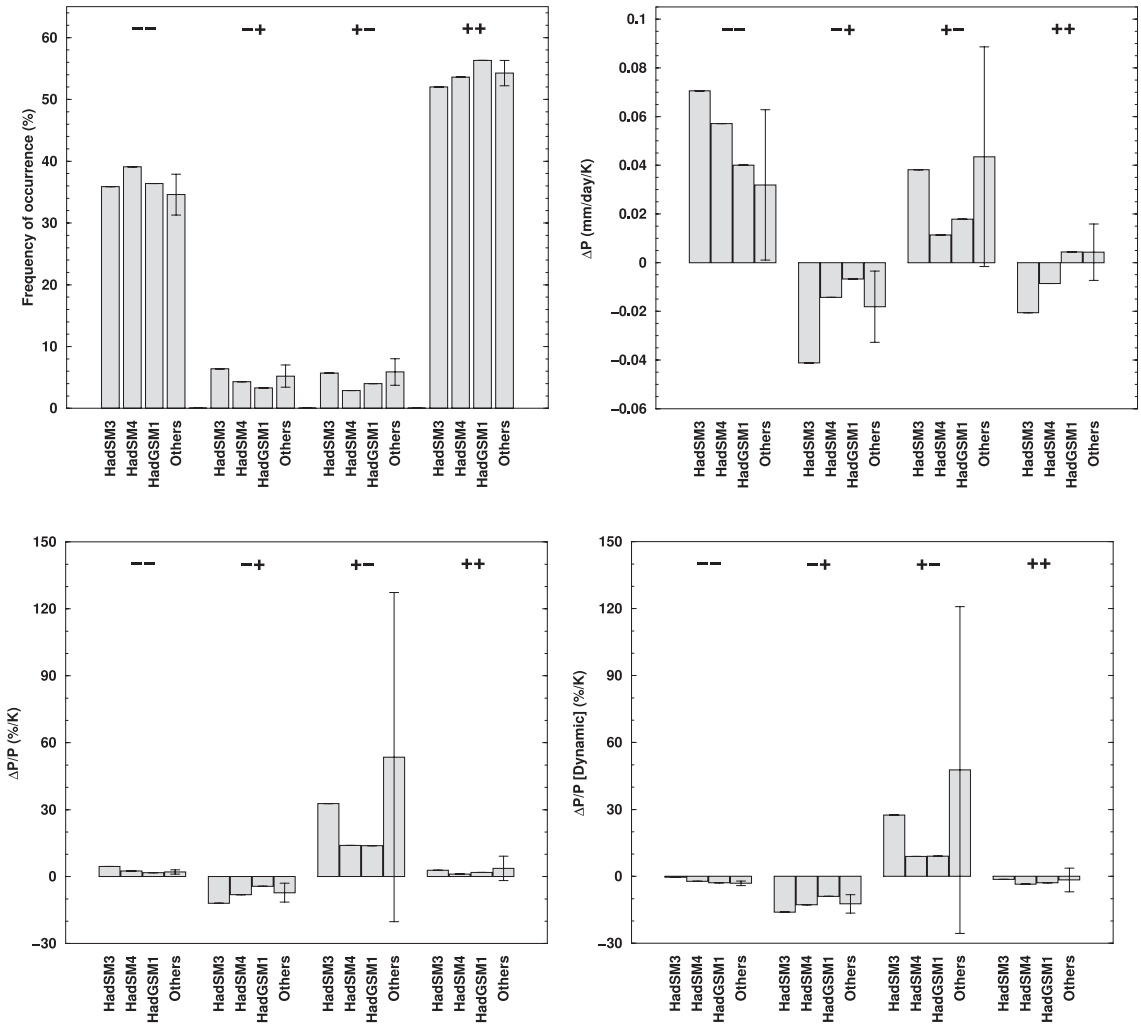

Figure 5. For all oceanic points between 30° N and 30° S: (top left) the areal coverage, as a fraction of the total area of the tropical oceans, for each of the circulation regimes defined in the text; (top right) the changes in total precipitation between the 2 × CO_2 case and the control within each regime weighted by their areal coverage; (bottom left) the area-weighted percentage change, as a fraction of the control, in total precipitation for each regime; (bottom right) the area-weighted percentage change in dynamic precipitation for each regime. The Hadley Centre models are indicated individually, the darker bars marked 'Others' show the mean of the seven non-Hadley Centre CFMIP models together with the inter-model spread of one standard deviation. All quantities have been normalized by the appropriate global climate sensitivity.

responses. Reversal of 500 hPa pressure velocity is therefore expected to have a large proportional effect on tropical ocean precipitation changes under climate change.

Figure 5(d) shows the fractional change in the dynamical precipitation within each regime. For the regimes representing reversal of pressure velocity under climate change, it is clear that the changes to the dynamic precipitation closely track the changes to the total and are of the same sign. Therefore dynamical changes are mainly responsible for the increase in precipitation.

Regime ω^{--} in figure 5(b) and regime ω^{+-} in figures 5(b)–(d) clearly show very large inter-model variation. The black bars representing the non-Hadley Centre models in figure 5 have been recalculated including the results from HadSM3, HadSM4 and HadGSM1 and the spread is virtually unchanged. The large spread is mainly due the outlying results of the CCSM3 and IPSL model which show very much larger values (604% and 444% respectively in figure 5(c) for example). This large variation between models, particularly for regime ω^{+-} is interesting because the frequency of occurrence of each of the regimes is remarkably consistent between the models given their different formulations, parameterizations schemes and resolutions.

Regime ω^{--} occurs in regions which exhibit ascending motion in both the control and doubled CO_2 cases. However, within this regime, it is clearly possible for the ascending motion to have accelerated or decelerated under climate change. Figure 6 recasts the relevant parts of figures 5(c) and (d) to take account of these two distinct possibilities. Figure 6(a) shows that where ascending motion in the control accelerates under climate change, the fractional change in total precipitation is increased, as expected. The reverse is true for decelerated ascent; the resulting reduction in precipitation is less than that due to accelerated ascent, a feature which is

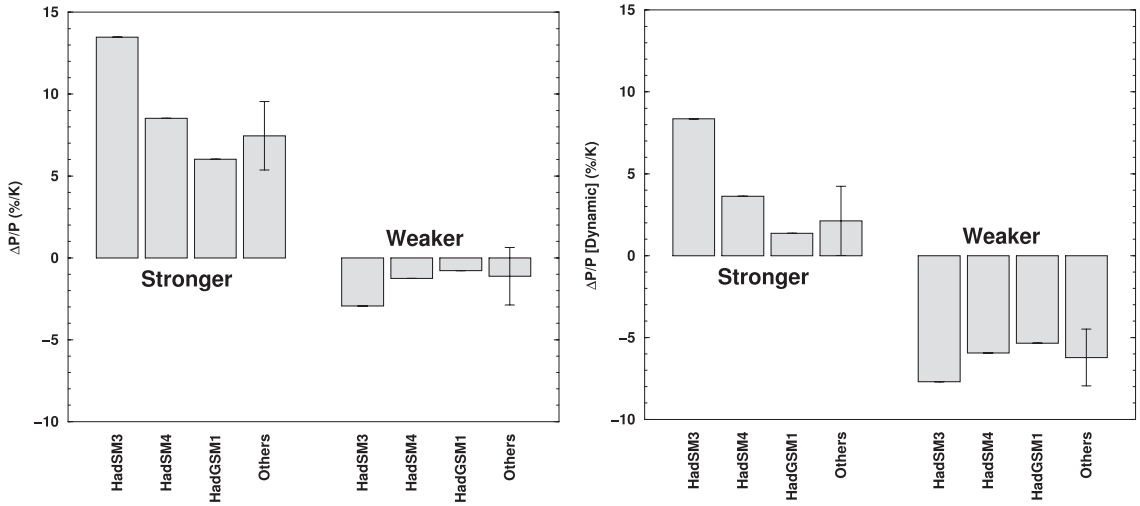

Figure 6. (Left) For the percentage change in total precipitation in regime ω^{--}, the first (second) set of four bars represents those areas where ascent strengthens (weakens) in the 2 × CO_2 case compared with the control. The order of each of the sets of four bars is as in figure 5. (Right) As before but for the dynamical precipitation changes.

particularly evident in the Hadley Centre models. Clearly, the small inter-model spread in figures 5(c) and (d) results from the cancellation between these increases and reductions in precipitation. However, the spread in these contributions is still far lower than that in the ω^{+-} regime.

5. Conclusions

The variability of precipitation in the atmospheric component of the HadGEM1 model have been validated against observational and reanalysis data. The main results are that the variability of the precipitation and 500 hPa pressure velocity are too high in the deep tropics and over the SPCZ although the spatial distribution of the quantities reproduces the validation data accurately. In addition to this, the strong correlation between precipitation and 500 hPa pressure velocity anomalies seen in the validation data is present in the model data also indicating a strong coupling between these two important elements of the hydrological cycle. The correlation between the sea surface temperature in the Nino 3.4 region with the local precipitation is well captured by the model, however the simulated local correlation is too strong. Some of this poor agreement between model and reanalysis data can be attributed to the sparse nature of extreme high latitude meteorological observations. Whilst it is certainly not self-evident that present day variability is directly analogous to behaviour under climate change this type of evaluation does help to identify potential strengths and weaknesses of the model and shed some light on its plausibility as a tool for examining climate change signals.

Comparing the total and dynamical precipitation changes between the perturbed climate case and a control climate case for three Hadley Centre models shows that noticeably different results are obtained. This is likely to be due to differences in boundary layer formulation, convective parameterization and dynamical core, and interactions between these schemes. The mean of the remaining members of the CFMIP ensemble show results which are noticeably different to the Hadley Centre models, however this average response is dominated by just two models, particularly in the equatorial Pacific Ocean. For the HadSM3 model, the changes in the total precipitation are almost entirely due to dynamical changes. However for HadSM4 and HadGSM1 and the remaining ensemble mean, although dynamical precipitation changes contribute the majority of the adjustments under climate change thermodynamic changes are also significant.

Partitioning the changes in 500 hPa pressure velocity between the control climate and a doubled CO_2 climate case into dynamical regimes has enabled isolation of the conditions under which the greatest changes in precipitation are to be expected. The areal coverage of the four regimes considered is remarkably consistent between all ten of the CFMIP models. This does not translate into common changes to the tropical oceanic precipitation however. It has been shown that although the regimes representing reversal of mid-tropospheric motion occur relatively infrequently, they have a large effect on the total precipitation change. In spite of this, there is significant cancellation between the absolute precipitation response in regimes ω^{-+} and ω^{+-}. Regime ω^{--} which indicates ascending motion in the control and perturbed climate cases gives the largest change to the precipitation, in the Hadley Centre models although the inter-model spread is large. Considering fractional precipitation changes, it is even clearer that the regimes showing reversal of sign of atmospheric motion are responsible for large changes in precipitation, with the regimes measuring unchanged ascending or descending motion showing small resulting changes. Computation of the dynamical precipitation response in regimes ω^{-+} and ω^{+-}, confirms that the majority of the precipitation changes are due to dynamical effects. Further partitioning regime ω^{--} into accelerating and decelerating regions shows that there is some cancellation in their respective effects on the precipitation change. The increase in precipitation due to accelerated ascent is dominant however, and the inter-model spread in both the increasing and decreasing regimes is smaller than in those

in which the sign of the mid-tropospheric vertical velocity reverses.

Acknowledgments

This work was supported by the Joint DECC and Defra Integrated Climate Programme, DECC/Defra (GA01101). The GPCP combined precipitation data were developed and computed by the NASA/Goddard Space Flight Centre's Laboratory for Atmospheres as a contribution to the GEWEX Global Precipitation Climatology Project and can be downloaded from http://www.esrl.noaa.gov/psd/data/gridded/data.gpcp.html. The HadCRUT3 data was obtained from www.hadobs.org. The ERA-40 reanalysis data can be obtained from www.ecmwf.int and the NCEP reanalysis data can obtained from http://www.esrl.noaa.gov/psd/data/gridded/data.ncep.reanalysis.html. CMAP data is can be obtained from http://www.esrl.noaa.gov/psd/data/gridded/data.cmap.html. We acknowledge the modelling groups, the Program for Climate Model Diagnosis and Intercomparison (PCMDI) and the WCRP's Working Group on Coupled Modelling (WGCM) for their roles in making available the WCRP CMIP3 multi-model dataset. Support of this dataset is provided by the Office of Science, US Department of Energy.

References

Adler R F, Gu G, Wang J-J, Huffman G J, Curtis S and Bolvin D 2008 *J. Geophys. Res.* **113** D22104
Adler R F *et al* 2003 *J. Hydro-meteorol.* B **4** 1147–67
Allan R P and Soden B J 2007 *Geophys. Res. Lett.* **34** L18705
Allan R P and Soden B J 2008 *Science* **321** 1481–4
Allen M R and Ingram W J 2002 *Nature* **419** 224–32
Bony S, Dufresne J-L, Le Treut H, Morcrette J-J and Senior C 2004 *Clim. Dyn.* **22** 71–86
Bony S, Lau K-M and Sud Y C 1997 *J. Clim.* **10** 2055–77
Brohan P, Kennedy J J, Harris I, Tett S F B and Jones P D 2006 *J. Geophys. Res.* **111** D12106
Emori S and Brown S J 2005 *Geophys. Res. Lett.* **32** L17706
Hartmann D L and Michelson M L 1993 *J. Clim.* **6** 2049–62
Held I M and Soden B J 2006 *J. Clim.* **19** 5686–99
John V O, Allan R P and Soden B J 2009 *Geophys. Res. Lett.* **36** L14702
Johns T C *et al* 2006 *J. Clim.* **19** 1327–53
Kalnay E *et al* 1996 *Bull. Am. Meteor. Soc.* **77** 437–71
Lock A P 2001 *Mon. Wea. Rev.* **129** 1148–63
Martin G M, Ringer M A, Pope V D, Jones A, Dearden C and Hinton T J 2006 *J. Clim.* **19** 1274–301
Parry M L *et al* (ed) 2007 Climate change 2007 impacts, adaptation and vulnerability *Contribution of Working Group 2 to the Fourth Assessment Report of the Intergovernmental Panel on Climate Change* (Cambridge: Cambridge University Press)
Pope V D, Gallani M L, Rowntree P R and Stratton R A 2000 *Clim. Dyn.* **16** 123–46
Solomon S *et al* (ed) 2007 Climate change 2007 the physical science basis *Contribution of Working Group 1 to the Fourth Assessment Report of the Intergovernmental Panel on Climate Change* (Cambridge: Cambridge University Press)
Trenberth K E, Caron J M, Stepaniak D P and Worley S 2002 *J. Geophys. Res.* **107** 4065
Trenberth K E and Shea D J 2005 *Geophys. Res. Lett.* **32** L14703
Uppala S M *et al* 2005 *Q. J. R. Meteor. Soc.* **131** 2961–3012
Vecchi G A and Soden B J 2007 *J. Clim.* **20** 4316–40
Vecchi G A, Soden B J, Wittenberg A T, Held I M, Leetmaa A and Harrison M J 2006 *Nature* **441** 73–6
Webb M, Senior C, Bony S and Morcrette J-J 2001 *Clim. Dyn.* **17** 905–22
Xie P and Arkin P A 1997 *Bull. Am. Meteor. Soc.* **78** 2539–58